Roland T. Loto[1, 2*]

[1]Department of Mechanical Engineering, Covenant University, Ota, Ogun State, Nigeria
[2]Department of Chemical, Metallurgical & Materials Engineering, Tshwane University of Technology, Pretoria, South Africa

***Corresponding author:** tolu.loto@gmail.com

Recibido: 13 de Agosto de 2016. Aceptado: 22 de Noviembre de 2016.

Corrosion inhibition studies of the combined admixture of 1,3-diphenyl-2-thiourea and 4-hydroxy-3-methoxybenzaldehyde on mild steel in dilute acid media

Abstract

The electrochemical corrosion inhibition properties of the combined admixture of 1,3-diphenyl-2-thiourea and 4-hydroxy-3-methoxybenzaldehyde on mild steel in 1 M H_2SO_4 and HCl acid media were studied through weight loss analysis, potentiodynamic polarization method, optical microscopy and IR spectroscopy. Results showed that the organic mixture effectively inhibited the corrosion of mild steel in both solutions with an optimal inhibition efficiency of 97.4% and 97.47% in H_2SO_4 from weight loss and potentiodynamic polarization test, while the corresponding values in HCl were 94.71% and 89.73% respectively. Thermodynamic calculations showed that the compound chemisorbed onto the steel surface blocking the diffusion of corrosive anions. Observations from micro-analytical images confirmed the effective inhibition property of the compound and its presence on the surface topography of the steel. Infrared spectra revealed the presence of the functional groups of the organic compound responsible for corrosion inhibition. The adsorption of the compound was deduced to obey the Langmuir, Frumkin and Freundlich adsorption isotherm.

Keywords: adsorption, corrosion, mild steel, inhibitor, hydrochloric acid, sulphuric acid.

Estudios de inhibición de la corrosión de la mezcla combinada de 1,3-difenil-2-tiourea y 4-hidroxi-3-metoxibenzaldehido en acero dulce en medio ácido diluido

Resumen

Se estudiaron las propiedades de inhibición de la corrosión electroquímica de la mezcla combinada de 1,3-difenil-2-tiourea y 4-hidroxi-3-metoxibenzaldehído sobre acero dulce en medios de H_2SO_4 y HCl 1 M mediante análisis de pérdida de peso, método de polarización potenciodinámica, microscopía óptica y espectroscopia IR. Los resultados mostraron que la mezcla inhibe eficazmente la corrosión del acero dulce en ambas soluciones con una eficacia de inhibición óptima de 97,4% y 97,47% en H_2SO_4, mientras que los valores correspondientes al HCl son 94,71% y 89,73%. Los cálculos termodinámicos demostraron que el compuesto quimiosorbido sobre la superficie de acero bloquea la difusión de aniones corrosivos. Las imágenes micro-analíticas confirmaron la efectiva propiedad de inhibición del compuesto y su presencia en la topografía superficial del acero. Los espectros infrarrojos revelaron la presencia de los grupos funcionales del compuesto orgánico responsable de la inhibición de la corrosión. La adsorción del compuesto se dedujo siguiendo las isotermas de adsorción de Langmuir, Frumkin y Freundlich.

Palabras clave: adsorción, corrosión, acero dulce, inhibidor, ácido clorhídrico, ácido sulfúrico.

Estudos de inibição da corrosão da mistura combinada de 1,3-difenil-2-tioureia e 4-hidroxi-3-metoxibenzaldeído em aço macio em meio ácido diluído

Resumo

Estudaram-se as propriedades de inibição da corrosão eletroquímica da mistura combinada de 1,3-difenil-2-tioureia e 4-hidroxi-3-metoxibenzaldeído em aço macio em meios de H_2SO_4 e HCl 1 M através de análise de perda de peso, método de polarização potenciodinâmica, microscopia óptica e espectroscopia de IV. Os resultados mostram que a mistura inibiu eficazmente a corrosão de aço macio em ambas as soluções com uma eficiência de inibição óptima de 97,4% e 97,47% em H_2SO_4, enquanto os valores correspondentes ao HCl são respectivamente 94,71% e 89,73%. Os cálculos termodinâmicos mostram que o composto quimisorvido sobre a superfície de aço bloquea a difusão de aniões corrosivos. As imagens micro-analíticas confirmam a propriedade de inibição do composto e sua presença na topografia superficial do aço. Os espectros de infravermelho revelaram a presença dos grupos funcionais do composto orgânico responsáveis pela inibição da corrosão. A adsorção do composto foi deduzida seguindo às isotermas de adsorção de Langmuir, Frumkin e Freundlich.

Palavras-Chave: adsorção, corrosão, aço macio, inibidor, ácido clorídrico, ácido sulfúrico.

Rev. Colomb. Quim. **2017**, *46* (1), 20-32. DOI: http://dx.doi.org/10.15446/rev.colomb.quim.v1n1.59578

Introduction

Mild steel is one of the most applicable construction materials, extensively used in chemical, petroleum, automotive, energy generating and allied industries for applications that are exposed to acids, alkalis and salty environments such as acid cleaning, pickling, descaling, industrial acid cleaning, cleaning of oil refinery equipment, heat exchangers and oil well acidizing (*1*). It is the cheapest, most common and most versatile form of steel serving for every application that requires huge amount of steel as it provides material properties that are acceptable for many applications. However it is weakly resistant to pitting and general corrosion, thus, it is continually replaced after being severely degraded in the corrosive environment during application.

Corrosion represents a significant cost burden and major industrial setback to the economy of every country; it is the largest single cause of plant and equipment breakdown in process industries. For a variety of industrial applications, it is possible the selection of construction materials which are completely resistant to corrosion from corrosive fluids, but the cost of such an approach is most often restrictive (*2*). Current reviews show that the most realistic cost of corrosion could be as high as 3% of the gross domestic product (GDP) of countries which have significant corrosion control measures in place (*3*, *4*). Numerous research and field experience over the decades have developed effective chemical treatments and corrosion control in so many applications from the transport of petrochemical products to the mining and processing of refractory ores. Despite the knowledge acquired, it is evident that there is a gap in information of applications in more challenging environments and in the development and application of novel chemical compounds and treatment practices. The chemicals, known as corrosion inhibitors, are continually fed into aqueous environments with the objective reacting with the metal surface to produce a passive protective chemical film (*5-7*).

The mechanism of inhibitor adsorption and the relationship between inhibitor molecular structures and their adsorption properties is of great importance in corrosion inhibition studies (*8*). Chemical compounds with functional groups containing heteroatoms within their molecular structure are capable of donating lone pair of electrons, important attribute of organic compounds in metal corrosion inhibition.

The use of organic compounds for corrosion inhibition of ferrous alloys in different acidic medium has been studied by different authors. The corrosion inhibiting property of these compounds is attributed to their molecular structure (*9-11*). Bouklah *et al.* (*12*) and Bentiss *et al.* (*13*) showed that the adsorption of organic inhibitors mainly depends on physicochemical and electronic characteristics of the inhibitor molecule, associated with their functional groups, steric effects, electron density of donor atoms, and the π-orbital character of donating electrons. A good inhibitor decreases the anodic and/or cathodic reaction of the corrosion process, the transport rate of the corrosive anions to the surface of the metal, and the potential difference at various sites on the metal surface. Inhibitors are basically easy to apply and offer the advantage of *in-situ* application.

To further contribute to the study of the use of low cost chemical compounds for corrosion inhibition of ferrous alloys and deeper understanding of their inhibition mechanism, this research aimed to investigate the inhibiting influence of the synergistic effect of 4-hydroxy-3-methoxybenzaldehyde and 1,3-diphenyl-2-thiourea on mild steel corrosion in 1 M H_2SO_4 and HCl acid solution through weight loss analysis, potentiodynamic polarization test and optical microscopy.

Materials and Methods

Material

Mild steel was purchased from the Steel Works, Owode, Nigeria and analyzed at the Materials Characterization Laboratory, Department of Mechanical Engineering, Covenant. This mild steel gave an average nominal composition of nominal per cent (w/w %) composition, shown in Table 1. The steel had a cylindrical dimension of 16 mm diameter.

Table 1. Nominal composition percentage of mild steel.

Element Symbol	C	Si	Mn	P	S	Cu	Ni	Al	Fe
% Composition (*w/w*)	0.401	0.169	0.440	0.005	0.012	0.080	0.008	0.025	98.86

Inhibitor

Combined mixture of 1,3-diphenyl-2-thiourea and 4-hydroxy-3-methoxybenzaldehyde (VTU), a solid white powdery substance obtained in synthesized form from SMM Instrument, South Africa was the inhibiting compound mixture used. Their structural formulas are shown in Figure 1, and the properties in Table 2.

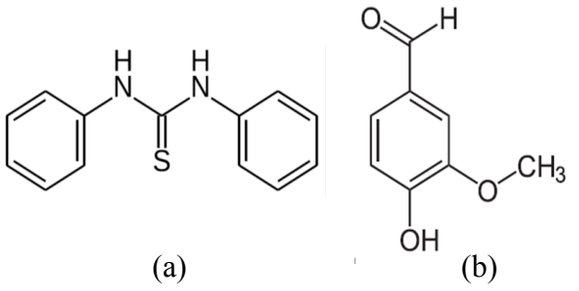

Figure 1. Chemical structure of (a) 1,3-diphenyl-2-thiourea (b) 4-hydroxy-3-ethoxybenzaldehyde.

Table 2. Chemical properties of the inhibiting compounds.

Compound	Molecular Formula	Molar Mass (g/mol)
1,3-diphenyl-2-thiourea	$C_{13}H_{12}N_2S$	228.31
4-hydroxy-3-methoxybenzaldehyde	$C_8H_8O_3$	152.15

VTU was prepared in different molar concentrations of 3.29 x 10^6 M, 6.57 x 10^6 M, 9.86 x 10^6 M, 1.31 x 10^5 M, 1.64 x 10^5 M and 1.97 x 10^5 M respectively per 200 mL each of the test media.

Acid test media

1 M HCl and H_2SO_4 acid media were prepared by dilution of an analytical grade H_2SO_4 (98% *w/w*) and HCl (37% *w/w*) with distilled water and used as the corrosive test environment.

Preparation of mild steel samples

The mild steels were machined into 14 test samples test specimens with an average length of 5 mm and a diameter of 15 mm. The two exposed surface ends of the cylindrical rod were metallographically prepared with silicon carbide abrasive papers of 80, 120, 220, 800 and 1000 grits, before being polished with 6 µm to 1 µm diamond liquid, rinsed with distilled water and acetone, dried and later stored in a desiccator for weight-loss analysis, open circuit potential measurement and potentiodynamic polarization resistance technique.

Weight-loss analysis

Weighed steel samples were individually immersed entirely into 200 mL of the dilute acid media for 432 h at ambient temperature of 25 °C. Each sample was removed from the solution at 24 h interval, rinsed with distilled water and acetone, dried and re-weighed according to ASTM NACE/ASTMG31-12a (*14*). Graphical illustrations of corrosion rate, ɤ (mm/yr) and percentage inhibition efficiency (η) versus exposure time T were plotted from the data obtained during the exposure hours. The corrosion rate (ɤ) calculation is defined as [1] (*15*).

$$ɤ = \left[\frac{87.6\tilde{\omega}}{DAT}\right] \quad [1]$$

Where $\tilde{\omega}$ is the weight loss in mg, *D* is the density in g/cm^3, *A* is the total area in cm^2 and 87.6 is a constant.

Inhibition efficiency (η) was calculated from [2].

$$\eta = \left[\frac{\tilde{\omega}_1 - \tilde{\omega}_2}{\tilde{\omega}_1}\right] \times 100 \quad [2]$$

Where $\tilde{\omega}_1$ and $\tilde{\omega}_2$ aη the weight loss with and without specific concentrations of VTU; η was calculated at all VTU concentrations throughout the exposure period.

Surface coverage is determined from [3] (*16, 17*)

$$\theta = \left[1 - \frac{\tilde{\omega}_2}{\tilde{\omega}_1}\right] \quad [3]$$

Where θ is the amount of VTU mixture, adsorbed per gram of the mild steel; $\tilde{\omega}_1$ and $\tilde{\omega}_2$ are the weight loss of the mild steel coupon with and without predetermined concentrations of VTU in the acid solutions.

Potentiodynamic polarization technique

Potentiodynamic polarization test was performed with cylindrical mild steel electrodes mounted in acrylic resin with an unconcealed surface area of 154 mm^2. The steel electrode was prepared according to ASTM G59-97(2014) (*18*). The studies were performed at 25 °C at ambient temperature with Digi-Ivy DY2300 potentiostat and electrode cell containing 200 mL of the acid media, with and without VTU mixture. Platinum was used as the counter electrode and silver chloride electrode (Ag/AgCl) was employed as the reference electrode. Potentiodynamic measurement was performed from -1.5V to +1.5 V at a scan rate of 0.0016 V/s according to ASTM G102-89 (2015) (*19*). The corrosion current density (j_{corr}) and corrosion potential (E_{corr}) were calculated from the Tafel plots of potential versus log current. The corrosion rate (ɤ) and the percentage inhibition efficiency (η_2) were from equation [4].

$$ɤ = \frac{0.00327 \times J_{corr} \times E_q}{D} \quad [4]$$

Where j_{corr} is the current density in µA/cm^2; D is the density in g/cm^3; Eq is the specimen equivalent weight in grams. 0.00327 is a constant for corrosion rate calculation in mm/yr (*20, 21*).

The percentage inhibition efficiency (η_2) was calculated from corrosion rate values using the equation [5].

$$\eta_2 = 1 - \left[\frac{ɤ_2}{ɤ_1}\right] \times 100 \quad [5]$$

Where $ɤ_1$ and $ɤ_2$ are the corrosion rates with and without VTU inhibitor.

Optical microscopy characterization and infrared spectroscopy

Optical micrographs of the surface morphology and topography of the uninhibited and inhibited mild steel sample was studied after weight-loss analysis with the aid of Omax trinocular optical metallurgical microscope at the Physical Metallurgical Laboratory, Covenant University, Ogun state, Nigeria. The VTU/acid solution, before and after the weight loss test were exposed to a range of infrared ray beams from Bruker Vertex 70/70v spectrometer. The transmittance and reflectance of the infrared rays at different frequencies was translated into an IR absorption plot consisting of spectra peaks. The spectral pattern was analyzed and matched according to IR absorption table to identify the functional group contained in the compound.

Adsorption Isotherm

Adsorption mechanisms are surface phenomenon by which multi-component solutions diffuse towards the surface of metallic alloys and adhere through physical or chemical adsorption at a constant temperature and pH (*22, 23*). To further understand the mechanism of interaction between the organic compound and metallic alloy, the adsorption behavior of the organic compound on the metal surface was delineated (*24*). Langmuir, Freundlich and Frumkin isotherms had the best fits for the data obtained for VTU in H_2SO_4 and while in HCl only Langmuir produce the best fit.

The isotherms are of the general form [6]

$$kc = g(\theta,x)\exp(-f\theta) \quad [6]$$

where g(θ,x) is the configurational factor subject to the physical model and assumptions involved in the emanation of the isotherms. The general form of the Langmuir equation is [7]:

$$[\frac{\theta}{1-\theta}] = K_{ads}C \quad [7]$$

rearranging equation [7], [8] results:

$$[\frac{c}{\theta} = \frac{1}{\theta}] + C \quad [8]$$

where θ is the value of surface coverage on the steel alloy, C is VTU concentration in the acid solution, and K_{ads} is the equilibrium constant of the adsorption process.

Frumkin isotherm assumes unit coverage at high inhibitor concentrations and that the electrode surface is inhomogeneous, i.e., the lateral interaction effect is not negligible. In this way, onlythe active surface of the electrode, on which adsorption occurs, is taken into account. Frumkin adsorption isotherm can be expressed according to equation [9].

$$\text{Log } \{C \times (\frac{\theta}{1-\theta})\} = 2.303 \log K + 2\alpha\theta \quad [9]$$

Where K is the adsorption-desorption constant and α is the lateral interaction term describing the interaction in adsorbed layer.

Freundlich isotherm states the quantitative relationship of the inhibiting compound and the molecular concentration of inhibitor molecules absorbed onto the steel which varies at specific concentrations according to equations [10] and [11] (*25*).

$$\theta = K_{ads}C^{n} \quad [10]$$

$$\log\theta = n \log C + \log K_{ads} \quad [11]$$

Where n is a constant subject to the properties of the adsorbed molecule; $0 < n < 1$, K_{ads} is the adsorption-desorption equilibrium constant connoting the interaction strength within the adsorbed layer. Absolute and higher results of K_{ads} suggest strong interaction between the organic molecule and the metal surface.

Results and discussion

Weight-loss measurements

Results for weight loss (ω̃), corrosion rate (ɤ) and percentage inhibition efficiency (ɲ) for VTU mixture and mild steel from the weight loss experiments in H2SO4 and HCl are presented in Tables 3 and 4. Figures 2 (a, b) and 3 (a, b) show the graphical illustration of corrosion rate and percentage inhibition efficiency versus exposure time in the acid media. The results for weight loss, corrosion rate and inhibition efficiency in both acid solutions are generally similarindicating similar electrochemical reaction. VTU mixture displayed similar corrosion inhibition characteristics on the redox electrochemical process basically through adsorption. Its presence in the acid media stifled the oxygen reduction, hydrogen evolution and oxidation reaction mechanism responsible for corrosion

Adsorption of VTU molecules onto the mild steel surface blocked the active sites where the dissolution and release of metal cations into the solution occurs as a result of the action of sulphates and chloride anions. The surface charge on metal oxides in contact with aqueous solutions arises from structural charge associated with the terminal oxygen and metal atoms at the mineral surface that have unsatisfied valence, as well as ions from the solution that associate with these terminal atoms in order to saturate this unsatisfied valence (*26*).

The reduction process was inhibited through increase in surface impedance of the steel whereby the dissociated hydrogen ions are unable to recombine to give of hydrogen gas. The presence of hydrogen on the metallic surfaces significantly accelerates their deterioration because hydrogen diffuses into the metal degrading their mechanical and chemical properties. The high corrosion rate and rate of hydrogen evolution for 0% VTU can be rationalized on the basis that H_2SO_4 and HCl react with mild steel and forms metal sulphates and chlorides, which are soluble in aqueous media. VTU inhibits the electrochemical reaction involving the release of atomic hydrogen (*27*). Figures 2(a) and (b) show a steady increase in corrosion rate for the mild steel sample in 0% VTU acid solutions till the end of the exposure period. However, with the addition of specific VTU concentrations the corrosion rates decline drastically with minimal values till the end of the experiment. The same phenomenon is observed in Figures 3 (a) and (b) for the inhibition efficiency values. The values ranged from 96.0-97.4% in H_2SO_4 and 96.2-97.2% in HCl.

VTU belongs to the group of organic compounds consisting of electron rich heteroatoms which are centers of Lewis acid-base interaction with the steel (*28*). They act by forming a protective film over the entire exposed area of the steel. The film chemisorbs onto the steel inhibiting the reaction of corrosive anions with the steel (*29*). This prevents the passage of metallic cations consisting of Fe^{2+} into the solution. The values of surface coverage (Tables 3 and 4) show that virtually the entire sample area were covered. This is due to the fact that the surface coverage of the VTU cations on the steel through adsorption increases with the increase in concentration (*30*). The VTU cations adhere themselves onto the steel surface through adsorption in the acid solution inhibiting the electrochemical reactions responsible for the deterioration of the steel.

The chemisorb adsorption is due to the donor–acceptor interaction between electrons of donor atoms and reactive sites of the inhibitors and the acceptor. Adsorption onto the steel surface can also be in the form of positively charged species which interact electrostatically with the metal cations and preadsorbed chlorides and sulphates (*31*). Visual observation of the steel samples in the test solutions can deduce that cathodic inhibition plays a significant role in the inhibition characteristics of VTU. Comparison of the uninhibited carbon steels (0% VTU) in H_2SO_4 and HCl solution with the inhibited solutions (0.13-0.75% VTU) in Tables 3 and 4 evidently shows that VTU at all concentrations effectively reduced the corrosion rates of the steel, thus protecting it.

Table 3. Results for mild steel in 1 M H_2SO_4 at predetermined concentrations of VTU.

Samples	Weight Loss (g)	Corrosion Rate (mm/yr)	VTU Inhibitor Concentration (%)	VTU Inhibitor Concentration (M x 10^{-3})	VTU Inhibition Efficiency (%)	Surface Coverage (θ)
A	7.5415	0.0292	0	0	0	0
B	0.3037	0.0012	0.13	3.29 x 10^{-6}	96.0	0.960
C	0.2726	0.0011	0.25	6.57 x 10^{-6}	96.4	0.964
D	0.2233	0.0009	0.38	9.86 x 10^{-6}	97.0	0.970
E	0.1937	0.0007	0.50	1.31 x 10^{-5}	97.4	0.974
F	0.1933	0.0007	0.63	1.64 x 10^{-5}	97.4	0.974
G	0.2076	0.0008	0.75	1.97 x 10^{-5}	97.2	0.972

Table 4. Results for mild steel in 1 M HCl at predetermined concentrations of VTU.

Samples	Weight Loss (g)	Corrosion Rate (mm/yr)	VTU Inhibitor Concentration (%)	VTU Inhibitor Concentration (M x 10^{-3})	VTU Inhibition Efficiency (%)	Surface Coverage (θ)
A	8.9772	0.0347	0		0	0
B	0.3045	0.0012	0.13	3.29 x 10-6	96.6	0.966
C	0.3201	0.0012	0.25	6.57 x 10-6	96.4	0.964
D	0.3446	0.0013	0.38	9.86 x 10-6	96.2	0.962
E	0.4751	0.0018	0.50	1.31 x 10-5	94.7	0.947
F	0.2277	0.0009	0.63	1.64 x 10-5	97.5	0.975
G	0.211	0.0008	0.75	1.97 x 10-5	97.7	0.976

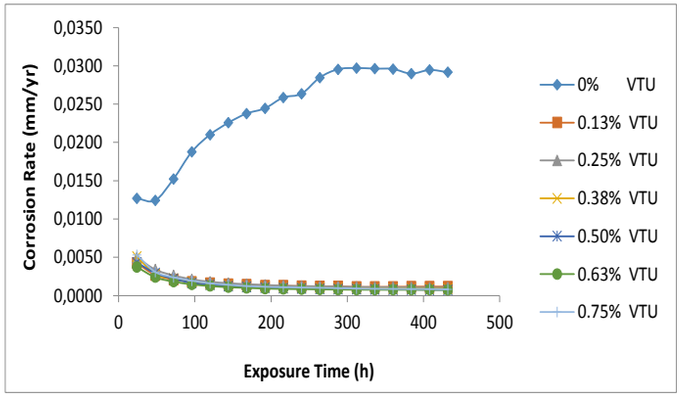

(a)

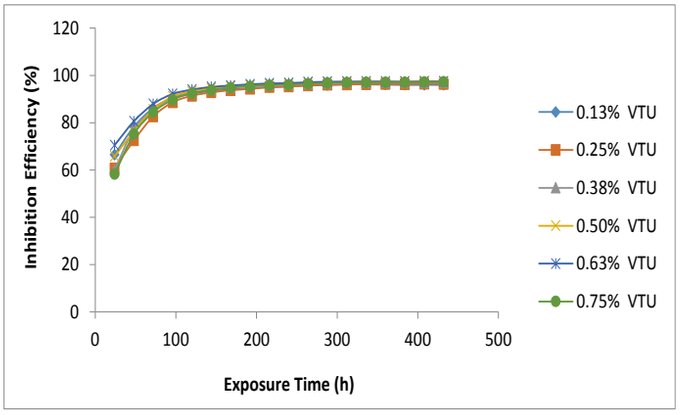

(b)

Figure 2. Graph illustration of (a) corrosion rate versus exposure time (b) inhibition efficiency versus exposure time in 1 M H_2SO_4.

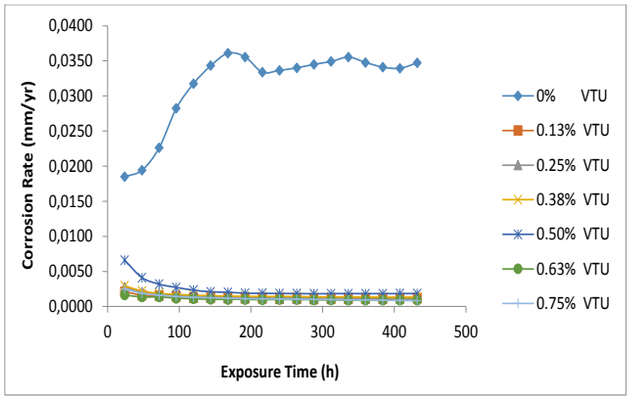

(a)

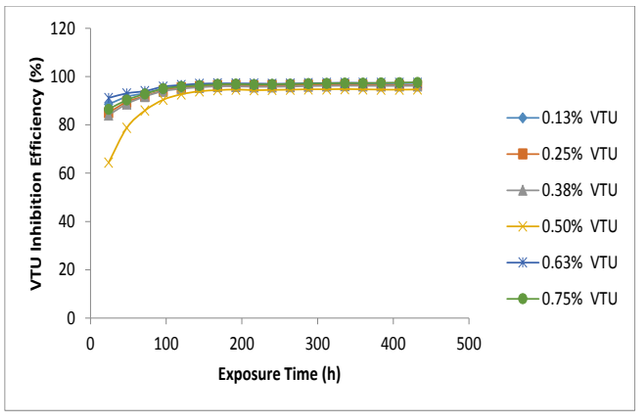

(b)

Figure 3. Graphical illustration of (a) corrosion rate versus exposure time (b) inhibition efficiency versus exposure time in 1 M HCl.

Adsorption Isotherm

The plots of $\frac{C}{\theta}$ versus the VTU concentration *C* were linear (Fig. 4 (a and b) indicating Langmuir adsorption. The divergence of the slope from unity in Figure 4(b) is due to VTU cations occupying specific adsorption sites at the metal/ion solution interface (*32, 33*). Figure 5 shows the Frumkin adsorption isotherm for VTU concentrations on the mild steel surface, the correlation factor is 0.7538. Figure 6 shows the Freundlich adsorption isotherm for VTU concentrations. Generally adsorption of organic molecules is a replacement reaction which involves the displacement of water molecules from the steel surface. During the corrosion inhibition process, the adsorption of organic molecules causes changes in the energy of interaction with water molecules which increases with increase in the energy of the reaction of the molecules. This in turn increases with increase in concentration of the inhibiting molecules.

Thermodynamics of the corrosion process

The quantity of metal loss due to corrosion deterioration is proportional to the degree of surface coverage of VTU mixture over the mild steel surface. It is suggested that the steel surface is covered with water dipoles, thus for adsorption of the cations of the organic compound to occur the water dipoles must be replaced by the cation in the electrochemical reaction as follows (*34, 35*).

$$nH_2O_{\text{electrode}} + \text{Organic}_{\text{solution}} \approx \text{Organic}_{\text{electrode}} + nH_2O_{\text{solution}} \quad [12]$$

As earlier mention in the discussion on adsorption isotherms, the thermodynamics of the replacement process is subject to the numbers of water molecules (n) displaced by VTU mixture. The values of the Gibbs free energy (ΔG^{o}_{ads}) for the adsorption process as shown in Tables 5 and 6 can be evaluated from equation [13].

$$\Delta G_{ads} = -2.303RT \log [55.5K_{ads}] \quad [13]$$

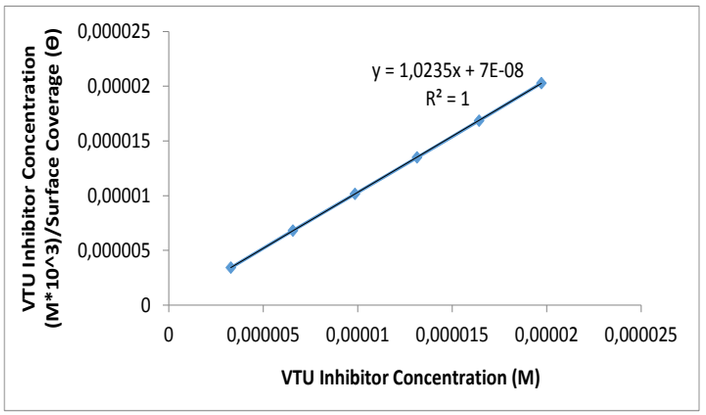

(a)

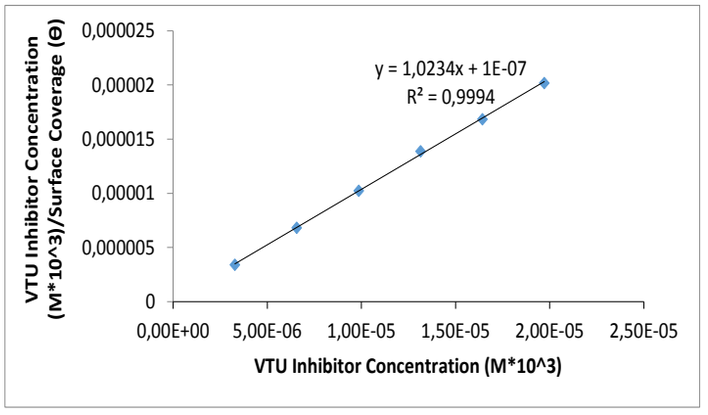

(b)

Figure 4. Plot of $\frac{C}{\theta}$ versus VTU concentration (C) (a) in 1 M H_2SO_4, (b) in 1 M HCl.

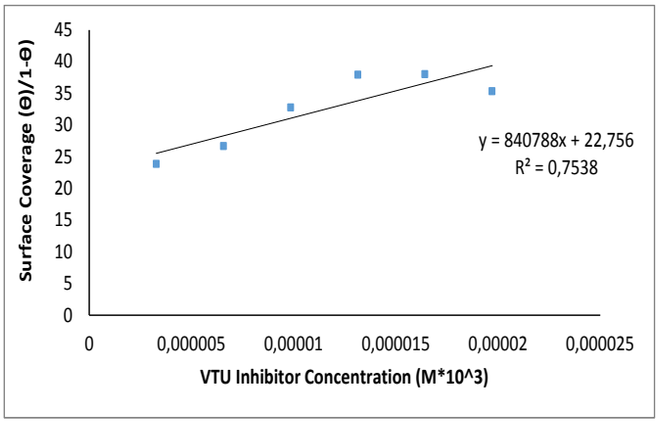

Figure 5. Frumkin isotherm model of VTU concentrations in 1 M H_2SO_4.

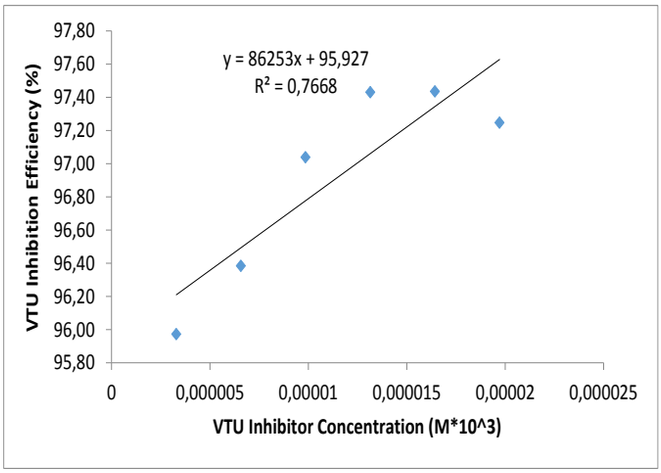

Figure 6. Freundlich isotherm model of VTU concentrations in 1 M H_2SO_4.

The heterogeneous characteristic (presence of flaws, impurities, cracks, vacancies, etc.) of the steel surface is responsible for the proportional relationship between the ΔG^{o}_{ads} of VTU and surface coverage (*34*, *36-37*). This relationship is caused by the changes in adsorption energies as shown in the tables. The negative values of ΔG^{o}_{ads} shows the adsorption is spontaneous. Values of ΔG^{o}_{ads} around -20 kJ/mol is consistent with physisorption reactions, while ΔG^{o}_{ads} around -40 kJ/mol is consistent with chemisorption reactions which basically involves charge sharing or transfer between the inhibitor cations and the valence electrons of the metal forming a co-ordinate covalent bond. The ΔG^{o}_{ads} values in H_2SO_4 ranged from -49.10 kJ/mol at 0.13% VTU to 45.63 kJ/mol at 0.75% VTU while in HCl the values ranged from -49.54 to -46.04 kJ/mol at 0.13-0.75% VTU. The high negative value of ΔG^{o}_{ads} shows that in H_2SO_4 and HCl acid medium chemisorption of VTU on the mild steel surface occurs (*38, 39*).

Table 5. Results for Gibbs free energy, surface coverage and equilibrium constant of adsorption for 0-7.5% VTU in 1 M H_2SO_4.

Samples	Surface Coverage (θ)	Equilibrium Constant of Adsorption (K)	Gibbs Free Energy (ΔG)
A	0	0	0
B	0.960	7253719.8	-49.10
C	0.964	4057998.1	-47.66
D	0.970	3325012.5	-47.17
E	0.974	2886467.7	-46.81
F	0.974	2314078.6	-46.27
G	0.972	1792071.7	-45.63

Table 6. Results for Gibbs free energy, surface coverage and equilibrium constant of adsorption for 0-7.5% VTU in 1 M HCl.

Samples	Surface Coverage (θ)	Equilibrium Constant of Adsorption (K)	Gibbs Free Energy (ΔG)
A	0	0	0
B	0.966	8668940.4	-49.54
C	0.964	4115814.1	-47.69
D	0.962	2541581.7	-46.50
E	0.947	1361696.0	-44.95
F	0.975	2339102.2	-46.29
G	0.976	2107544.0	-46.04

Potentiodynamic Polarization studies

The corrosion polarization behaviour of VTU inhibiting compound on mild steel in 1 M H_2SO_4 and HCl are shown in Figures 7 and 8. Tables 7 and 8 show the potentiodynamic data obtained. Table 6 shows the significant change in corrosion rate in the presence of VTU (0.13- 075% VTU) in comparison to the concentration without VTU. The corrosion rate decreased significantly at 0.15% VTU and continues to decrease progressively with increase in VTU concentration. The inhibition efficiency at the lowest VTU concentration (0.13% VTU) is 92.49%, the values continues to increase till 97.47% at 0.63% VTU, after which it decreased to 94.05% at 0.75% VTU. The results further confirm that VTU effectively inhibits the corrosion of mild steel in H_2SO_4 at all the concentrations studied. The corrosion current also decreased significantly. The inhibition efficiency of VTU is slightly dependent on the values of its concentration acid solution.

The same phenomenon was observed in Table 7 for the electrochemical influence of VTU in HCl, however the maximum inhibiting effect of VTU is 89.73% at 0.75% VTU. This shows that VTU molecules which protonates in the acid solutions is more effective inhibiting the diffusion of SO_4^{2-} anions compared to Cl^- anions, probably due to the small size of Cl^- ions which enables selective penetration through the protective film. The anodic and cathodic polarization plots in Figure 7 shows active-passive behavior in the presence of VTU inhibitor in H_2SO_4 media.

The plots displayed similar electrochemical behavior with the corrosion potential shifting majorly to anodic potentials suggesting that the mechanism of inhibition is through film formation by adsorption. This prevents the anodic dissolution and deterioration of the steel sample through surface coverage of the reaction sites. The coverage decreases the number of surface metal atoms at which corrosion reactions can occur. Anodic dissolution process of is considered to occur at specific dislocations in the metal surface, where metal atoms are less firmly held to their neighbors than in the plane surface. The anodic and cathodic Tafel slopes were moderately affected with changes in VTU concentration suggesting that the oxidation and reduction reactions were simultaneously inhibited however as earlier mentioned from corrosion potential values anodic inhibition tends to predominate.

The polarization plots in Figure 8 shows greater tendency for cathodic inhibition as observation of the corrosion potential values indicates a significant shift to negative potentials. This shows that the mechanism of inhibition in HCl is through stifling of the hydrogen evolution and oxygen reduction reactions whereby VTU cations selectively precipitates on the cathodic reaction sites increasing the surface impedance of the steel. The anodic and cathodic Tafel slopes remained generally the same at all VTU concentrations. The maximum change in corrosion potential in H_2SO_4 is 52 mV in the anodic direction while in HCl it is 34 mV in the cathodic direction, thus VTU is a mixed type inhibitor in both acids (*40, 41*).

Corrosion of metallic alloys is complex mechanism due to the presence of numerous anodic and cathodic reaction sites on the metal surface. VTU inhibitor interacts with the reaction sites retarding electrochemical corrosion reactions and preventing the diffusion of reactive corrosive species from solution through the metal solution interface. As earlier mentioned the heteroatoms of VTU mixture are the adsorption center for its interaction with the steel surface via electrostatic interaction between a negatively charged surface, through a specifically adsorbed anion (Cl^-) on the steel, and the cation molecule of VTU inhibitor (*42, 43*). VTU mixture has nitrogen, oxygen and sulphur atoms in its molecular structure and adsorption occurs through the formation of an iron–nitrogen coordinate bond or pi electron interaction between them (*44*).

Optical Microscopy Analysis

The micro-analytical images of the mild steel samples before and after corrosion are presented from Figures 9(a) to 10(d). Figures 9 (a)-(d) show the images of the steel samples before the corrosion test at magnifications of 4X, 10X, 40X and 100X. The image presents the samples as received after metallographic preparation of their surfaces. Figure 10(a-d) shows the micro-analytical image of the control specimens after the corrosion test. Topographic degradation and significant deterioration of the surface morphology of the sample is clearly visible as a result of the electrochemical action of corrosive anions present in the acid media. The anions react with the metal surface through the redox corrosion mechanism resulting in the loss of valence electrons and passage of Fe^{2+} cations into the acid solution.

Table 7. Potentiodynamic polarization results for mild steel in 1 M H_2SO_4.

Sample	Inhibitor Concentration (%)	Corrosion Rate (mm/yr)	Inhibition Efficiency (%)	Corrosion Current (A)	Current Density (A/cm^2)	Corrosion Potential (V)	Polarization Resistance, R_p (Ω)	Cathodic Tafel Slope, B_c (V/dec)	Anodic Tafel Slope, B_a (V/dec)
0	0	4.35	0	5.78×10^{-4}	3.75×10^{-4}	-0.327	44.44	-7.990	13.870
1	0.13	0.33	92.49	4.34×10^{-5}	2.82×10^{-5}	-0.334	59.25	-4.273	9.532
2	0.25	0.31	92.88	4.11×10^{-5}	2.67×10^{-5}	-0.292	49.01	-3.046	8.188
3	0.38	0.24	94.53	3.16×10^{-5}	2.05×10^{-5}	-0.277	81.29	-2.588	16.220
4	0.50	0.16	96.25	2.17×10^{-5}	1.41×10^{-5}	-0.275	118.60	-3.923	18.740
5	0.63	0.11	97.47	1.46×10^{-5}	9.49×10^{-6}	-0.311	175.80	-5.737	14.540
6	0.75	0.26	94.05	3.44×10^{-5}	2.23×10^{-5}	-0.290	74.72	-4.017	17.090

Table 8. Potentiodynamic polarization results for mild steel in 1 M HCl.

Sample	Inhibitor Concentration (%)	Corrosion Rate (mm/yr)	Inhibition Efficiency (%)	Corrosion Current (A)	Current Density (A/cm^2)	Corrosion Potential (V)	Polarization Resistance, Rp (Ω)	Cathodic Tafel Slope, Bc (V/dec)	Anodic Tafel Slope, Ba (V/dec)
0	0	5.60	0	7.44×10^{-4}	4.83×10^{-4}	-0.324	34.55	-8.639	11.270
1	0.13	0.82	85.40	1.09 x 10-^{4}	7.05×10^{-5}	-0.326	236.60	-6.933	9.942
2	0.25	0.80	85.76	1.06×10^{-4}	6.88×10^{-5}	-0.358	242.50	-7.834	10.380
3	0.38	0.83	85.11	1.11×10^{-4}	7.19×10^{-5}	-0.338	223.00	-7.057	10.730
4	0.50	0.80	85.75	1.06×10^{-4}	6.88×10^{-5}	-0.334	242.40	-6.005	10.150
5	0.63	0.67	87.96	8.96×10^{-5}	5.82×10^{-5}	-0.329	286.90	-6.286	10.130
6	0.75	0.58	89.73	7.64×10^{-5}	4.96×10^{-5}	-0.343	336.20	-8.287	10.580

This was clearly observed during the exposure hours whereby there was a gradual buildup of sediments of iron compounds and significant discoloration of the acid solution. Figures 10(a-d) also shows that mild steel is unsuitable for applications in such environments as rapid deterioration occurs. The image in Figure 10 contrasts the image in Figure 9.

The presences of large voids due to severe corrosion are visible since mild steel is known to undergo general corrosion. Figures 11 (a-d) shows the images of the mild steel specimens from the acid solution with VTU inhibiting compound after the corrosion test. Based on results from weight loss and potentiodynamic polarization, the images show the surface of well-protected steel specimens. VTU molecules acting through adsorption from electrostatic attraction covers and possibly builds up on the steel surface and reacting with it through the chemisorption mechanism to effectively protect the steel from corrosion. The images in Figure 11(a and b) are generally the same but closer magnification reveals the presence of the inhibiting compound which strongly adheres to the steel surface protecting it from deterioration.

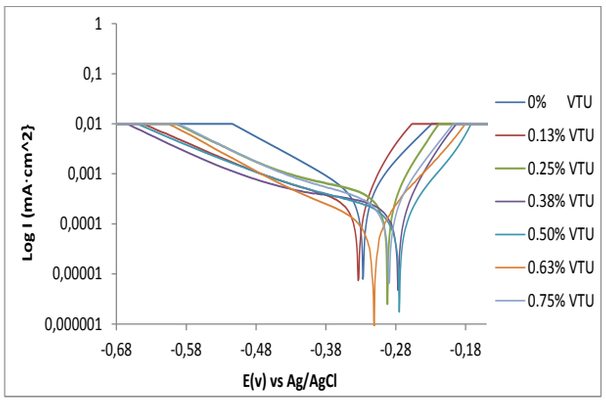

Figure 7. Anodic and cathodic polarization curve for mild steel in 1 M H_2SO_4 acid.

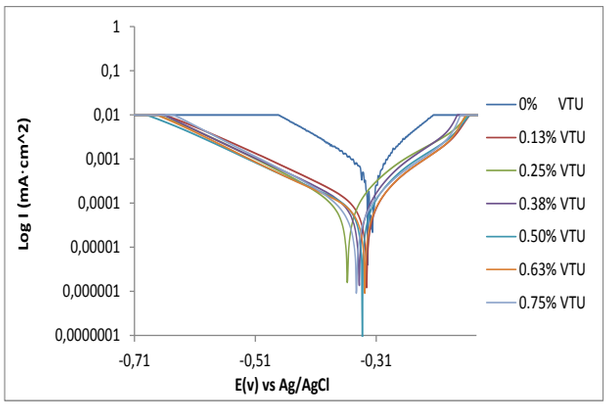

Figure 8. Anodic and cathodic polarization curve for mild steel in 1 M HCl acid.

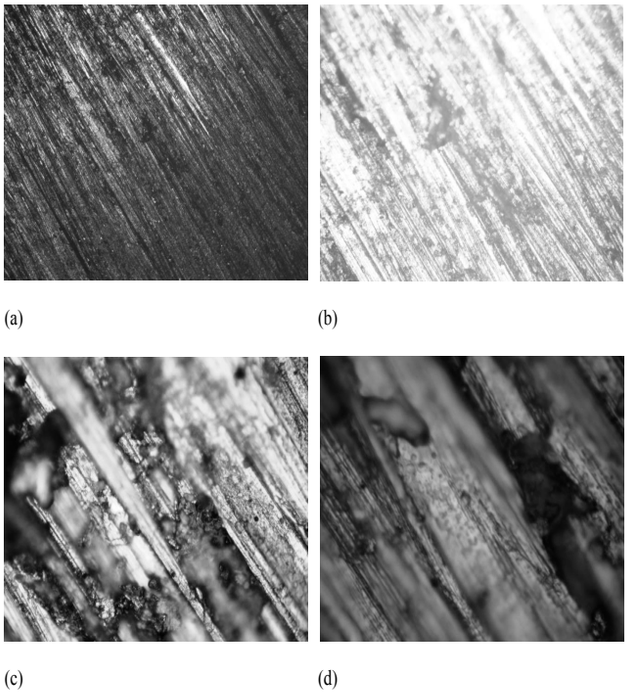

Figure 9. Microanalytical images of mild steel before corrosion (a) 4X, (b) 10X, (c) 40X, (d) 100X.

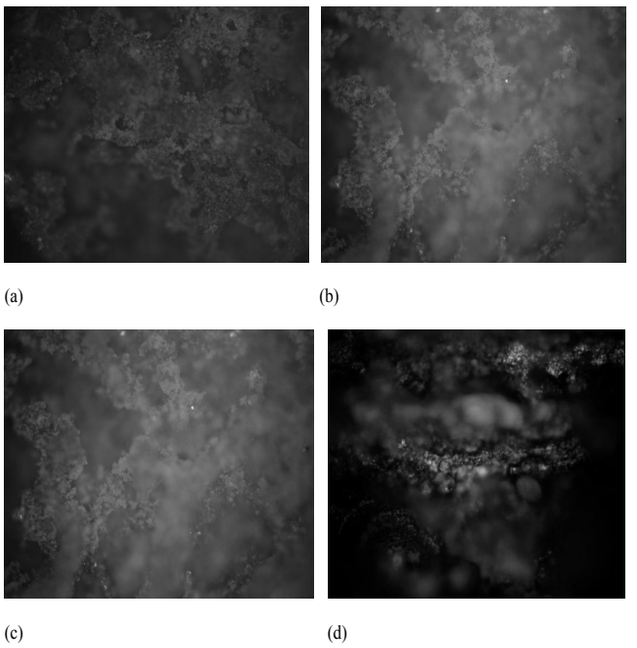

Figure 10. Microanalytical images of mild steel after corrosion without VTU mixture (a) 4X, (b) 10X, (c) 40X, (d) 100X.

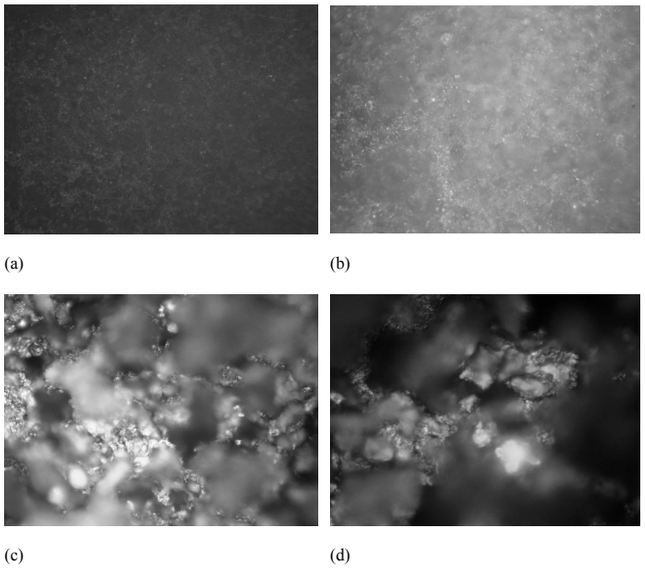

(a) (b)

(c) (d)

Figure 11. Micro-analytical images of mild steel after corrosion study with VTU mixture (a) 4X, (b) 10X, (c) 40X, (d) 100X.

IR spectroscopy

IR spectroscopy was used to study the properties and center of adsorption of VTU mixture within its molecular structure. Figures 12 (a) and (b) show the spectra peaks for VTU mixture in H_2SO_4 before and after the corrosion test (without and with the mild steel sample). Figure 12(c) shows the superimposition of Figures 12(a) and (b), while Figures 13(a) and (b) show the spectra peaks for VTU mixture in HCl before and after the corrosion test (without and with the mild steel sample). Superimposition of Figures 13(a) and (b) is shown in Figure 13(c).

Characteristic IR absorptions are presented in Table 9. Observation and comparison of Figure 12(a) with Table 9 shows the spectra peaks at 3345.78 cm^{-1} (N-H stretch bond), 1636.38 cm^{-1} (N-H bend bond), 1190.38 cm^{-1} (C–H wag (–CH_2X) bond) and 1050.08 cm^{-1} (C-N stretch bond). These consist of primary and secondary amines and amides, primary amines, aliphatic amines and alkyl halides functional groups. The comparison of Figure 12(b) with Table 9 shows similar functional groups with Figure 12(a) at spectra peaks of 3359.26, 1631.36, 1182.56, and 1047.57 cm^{-1}. Spectra peaks of 871.62 cm^{-1} (=C–H bend, N–H wag and C–H "oop" bonds) consists of alkenes, primary and secondary amines, and aromatics functional groups while spectra peak of 577.15 cm^{-1} (C–Cl stretch and C–Br stretch bonds) consists of alkyl halides functional groups.

Superimposition of Figures 12(a) and (b) in Figure 12(c) shows the differences between the VTU compounds involved in and not involved in the inhibition of mild steel samples in H_2SO_4. The decrease in transmittance for Figure 12(b) in comparison to Figure 12(a) shows that the functional groups earlier mentioned were actively involved in the inhibition of the steel by adsorption through chemisorption mechanism.

The groups are responsible for the formation of stable complex between the iron constituents and functional groups present in the VTU mixture forming covalent or coordinate bonds between the anionic components of VTU and vacant Fe d-orbital. The metal-inhibitor bond usually leads to corrosion inhibition through adsorption (*45*).

The corrosion retarding mechanism through stable complex formation dominates at all VTU concentrations. The corrosion retarding mechanism is due to strong adsorption resulting from the donation of lone pair of electrons on oxygen and nitrogen to vacant d-orbital of the metal which leads to the formation of metal complexes.

The spectra peaks of 3341.60 cm^{-1} (N-H stretch, O–H stretch and H–bonded bonds), 2094.47 cm^{-1} (–C(triple bond)C– stretch bond), 1632.32 cm^{-1} (N–H bend bond) and 1291.99 cm^{-1} (N–O symmetric stretch, C–N stretch, C–O stretch and C–H wag (–CH_2X) bonds) in Figures 13(a) and (b) consists of alcohols, phenols, primary, secondary amines and amides, alkynes and aromatics functional groups responsible for corrosion inhibition by VTU in HCl acid. However, super imposing Figures 13(a) and (b) in Figure 13(c) shows that the spectral diagrams are basically the same. It is suggested that VTU essentially inhibited the mild steel corrosion through film formation by blocking the active sites on the surface but not necessarily affecting the mechanism of the corrosion process.

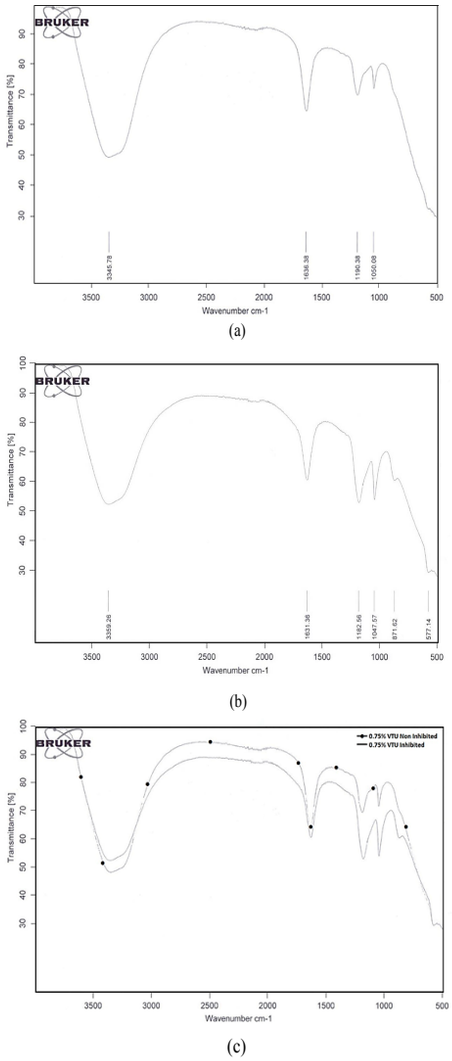

Figure 12. IR spectra of VTU inhibiting compound (a); VTU mixture in H_2SO_4 before mild steel corrosion (b); VTU mixture in H_2SO_4 after mild steel corrosion (c). Superimposition of Figures 11(a) and (b).

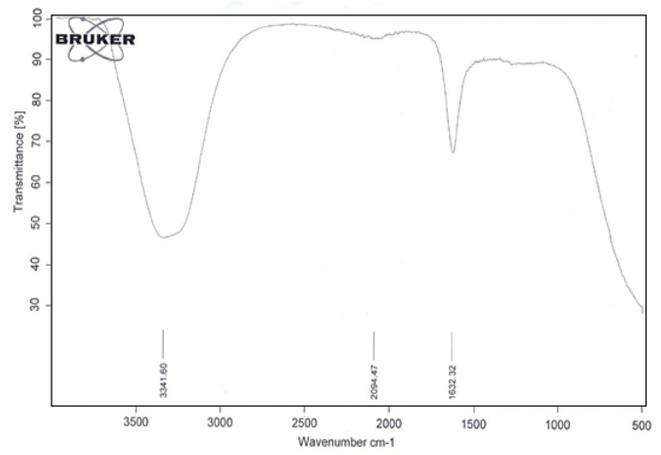

(a)

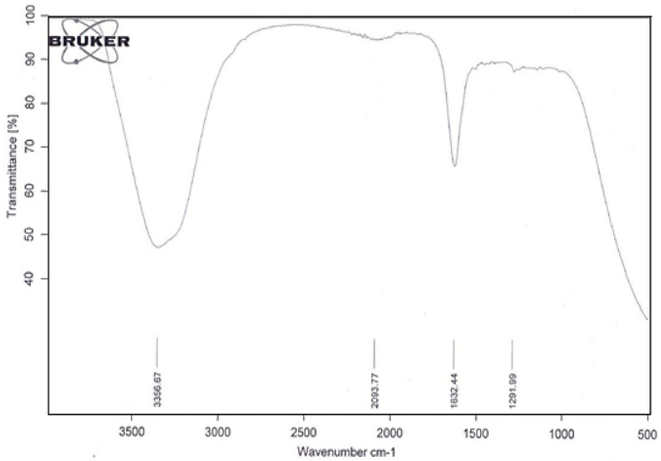

(b)

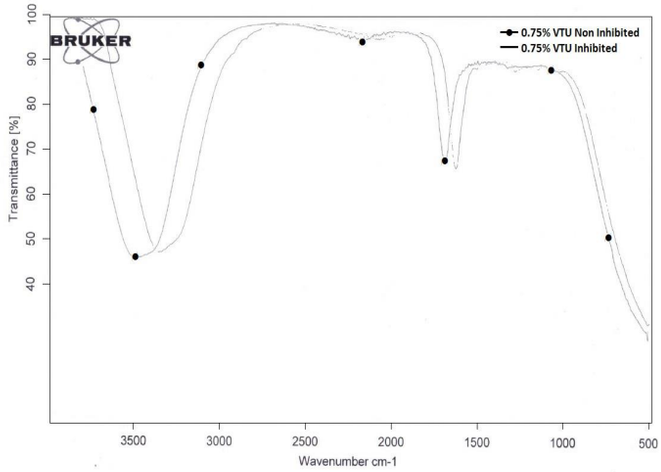

(c)

Figure 13. IR spectra of VTU inhibiting compound (a); VTU mixture in HCl before mild steel corrosion (b); VTU mixture in HCl after mild steel corrosion (c). Superimposition of Figures 12(a) and (b)

Table 9. Table of characteristic IR absorptions (Extracted).

Wavenumber (cm^{-1})	Bond	Functional Group
3400–3250 (m)	N–H stretch	primary, secondary amines, amides
3500–3200 (s,b)	O–H stretch, H–bonded	alcohols, phenols
2260–2100 (w)	–C (triple bond) C– stretch	alkynes
1650–1580 (m)	N–H bend	primary amines
1300–1150 (m)	C–H wag (–CH_2X)	alkyl halides
1360–1290 (m)	N–O symmetric stretch	nitro compounds
1335–1250 (s)	C–N stretch	aromatic amines
1320–1000 (s)	C–O stretch	alcohols, carboxylic acids, esters, ethers
1300–1150 (m)	C–H wag (–CH2X)	alkyl halides
1250–1020 (m)	C–N stretch	aliphatic amines
1000–650 (s)	=C–H bend	alkenes
910–665 (s, b)	N–H wag	primary, secondary amines
900–675 (s)	C–H "oop"	aromatics
850–550 (m)	C–Cl stretch	alkyl halides

m=medium, w=weak, s=strong, n=narrow, b=broad, sh=sharp

Conclusions

Corrosion inhibition study of VTU (1,3-diphenyl-2-thiourea and 4-hydroxy-3-ethoxybenzaldehyde) on mild steel in acidic environment was evaluated and the results showed that it is a potent inhibitor. VTU performed effectively with inhibition efficiencies above 90% at all concentrations evaluated in H_2SO_4 and HCl acid solutions. The inhibition characteristics of VTU was determined to be mixed type due to its influence on the redox electrochemical process, however it showed greater tendency for anodic inhibition in H_2SO_4 and cathodic inhibition in HCl acid. VTU being a mixture of organic compounds with heteroatoms protonates in the acid solution, forms cationic molecules which reacts with the charged steel surface, forming in turn a chemically adsorbed protective layer as shown from thermodynamic calculations. Infrared spectra confirmed the presence of functional groups of the organic compound responsible for corrosion inhibition. The adsorption mechanism aligned with Langmuir, Frumkin and Freundlich adsorption isotherms. The corrosion inhibition results were confirmed from micro-analytical images through optical microscopy. The difference in surface topography and morphology was clearly distinct.

Acknowledgement

The author is grateful to the Department of Mechanical Engineering, Covenant University for the provision of facilities for the research work.

References

1. Shetty, S.D.; Shetty, P.; Nayak, H.V.S. The inhibition action of N-furfuryl-N'-phenyl thiourea on the corrosion of mild steel in acid media. *J. Serb. Chem. Soc.* **2006**, *71*(10), 1073-1080. DOI: https://doi.org/10.2298/jsc0610073s.
2. Corrosion of carbon steel. http://www. http://www.totalmateria.com/articles/Art60.htm. [Accessed January 9, 2017]
3. Corrosion and preventative strategies in the United States. http://www.nace.org/uploadedFiles/Publications/ccsupp.pdf. [Accessed January 9, 2017]
4. Microbiologically influenced corrosion in fire sprinkler systems, Automatic sprinkler systems handbook. http://webcache.googleusercontent.com/search?q=cache:jkMPbYnMPaYJ:www.nfpa.org/~/media/files/formsapremiums/nf13hb07_chs3.Pdf+&cd=6&hl=en&ct=clnk. [Accessed March 10, 2016]
5. Toth J. *Adsorption: Theory, modeling, and analysis*. Marcel Dekker: New York, 2002.
6. Bentiss, F.; Traisnel, M.; Chaibi, N.; Mernari, B.; Vezin, H.; Lagrenee, M. 2,5-Bis(nmethoxyphenyl)-1,3,4-oxadiazoles used as corrosion inhibitors in acidic media: correlation between inhibition efficiency and chemical structure. *Corros. Sci*. **2002**, *44*(10),2271–2289. DOI: http://dx.doi.org/10.1016/S0010-938X(02)00037-9.
7. Punckt, C.; Bolscher, M.; Rotermund, H. H.; Mikhailov, A. S.; Organ, L.; Budiansky, N. *et al*. Sudden onset of pitting corrosion on stainless steel as a critical phenomenon. *Chem. Inform.* **2004**, *35*(44). DOI: https://doi.org/10.1002/chin.200444018.
8. Bentiss, F.; Traisnel, M.; Vezin, H.; Hildebrand, H.F.; Lagrenee, M. 2,5-Bis(4- dimethylaminophenyl)-1,3,4-oxadiazole and 2,5-bis(4-dimethylaminophenyl)-1,3,4-thiadiazole as corrosion inhibitors for mild steel in acidic media. *Corros. Sci*. **2004**, *46*(11), 2781– 2792. DOI: http://dx.doi.org/10.1016/j.corsci.2004.04.001.
9. Vosta, J.; Pelikanj, S. M. Practical aspects of corrosion, materials and corrosion. 1974; 750-756.
10. Sathiyanarayanan, S.; Balakrishanan, K.; Dhawan, S.K.; Trivedi. D.C. Prevention of corrosion of iron in acidic media using poly (o-methoxyl-aniline). *Electrochim. Acta.* **1994**, *39*(6), 831-837. DOI: http://dx.doi:10.1016/0013-4686(94)80032-4.
11. Zvauya, R.; Dawson, J.L. Electrochemical reduction of carbon dioxide and the effect of the enzyme carbonic anhydrase 11 on iron corrosion. *J. Chem. Technol. Biotechnol.* **1994**, *61*(4), 319–324. DOI: http://dx.doi:10.1002/jctb.280610406.
12. Boukla, M.; Benchat, N.; Hammouti, B.; Aouniti, A.; Kertit, S. Thermodynamic characterisation of steel corrosion and inhibitor adsorption of pyridazine compounds in 0.5 M H_2SO_4. *Mats. Lett.* **2006**, *60*(15), 1901-1905. DOI: http://dx.doi.org/10.1016/j.matlet.2005.12.051.
13. Bentiss, F.; Traisnel, M.; Lagrene, M. Influence of 2,5-bis(4-dimethylaminophenyl)-1,3,4-thiadiazole on corrosion inhibition of mild steel in acidic media. *J. of App. Elect*. **2001**, *31*(1), 41-48. DOI: http://dx.doi.org/10.1023/A:1004141309795.
14. ASTM NACE / ASTMG31 - 12a (2012), Standard Guide for Laboratory Immersion Corrosion Testing of Metals. http://www.astm.org/Standards/G31. (Accessed May 5, 2016)
15. Venkatesan, P.; Anand, B.; Matheswaran, P. Influence of formazan derivatives on corrosion inhibition of mild steel in hydrochloric acid medium. *E-J. of Chem*. **2009**, *6*(1), 438-444. DOI: http://dx.doi.org/10.1155/2009/507383.
16. Abbasova, V.M.; Abd El-Lateefa, H.M.; Aliyevaa, L.I.; Qasimova, E.E.; Ismayilova, I.T.; Khalaf, M.M. A study of the corrosion inhibition of mild steel C1018 in CO_2- saturated brine using some novel surfactants based on corn oil. *Egyptian J. of Pet.* **2013**, *22*(4), 451-470. DOI: http://dx.doi.org/10.1016/j.ejpe.2013.11.002.
17. Sethi, T.; Chaturvedi, A.; Mathur, R.K. Corrosion inhibitory effects of some schiff's bases on mild steel in acid media. *J. Chilean Chem. Soc.* **2007**, *3*(52), 1206-1213. DOI: http://dx.doi.org/10.4067/S0717-97072007000300003.
18. ASTM G59 – 97(2014), Standard Test Method for Conducting Potentiodynamic Polarization Resistance Measurements. http://www.astm.org/Standards/G31/. (Accessed: 30.05.2016)
19. 19. ASTM G102 - 89 e1 (2015), Standard Practice for Calculation of Corrosion Rates and Related Information from Electrochemical Measurements. http://www.astm.org/Standards/G31/, (Accessed: 30.05.2016).
20. Ahmad, K. Principles of corrosion engineering and corrosion control. Butterworth- Heinemann: Oxford, UK, 2006.
21. Choi, Y.; Nesic, S.; Ling, S. Effect of H2S on the CO2 corrosion of carbon steel in acidic solutions. *Electrochim. Acta.* **2011**, *56*, 1752-1760. DOI: http://dx.doi.org/10.1016/j.electacta.2010.08.049.
22. Limousin, G.; Gaudet, J.P.; Charlet, L.; Szenknect, S.; Barthes, V.; Krimissa, M. Sorption isotherms: a review on physical bases, modeling and measurement. *App. Geochem.* **2007**, *22*(2), 249–275. DOI: http://dx.doi.org/10.1016/j.apgeochem.2006.09.010.
23. Allen, S.J.; Mckay, G.; Porter, J.F. Adsorption isotherm models for basic dye adsorption by peat in single and binary component systems. *J. Colloid. Interf. Sci.* **2004**, *280*(2), 322-333. DOI: http://dx.doi.org/10.1016/j.jcis.2004.08.078.
24. Tosun, A.; Ergun, M. Protection of corrosion of carbon steel by inhibitors in chloride containing solutions. *Gazi University J. Sci.* **2006**, *19*(3), 149-154.
25. Foad El-Sherbini, E.E.; Abdel Wahaab, S.M.; Deyab, M. Ethoxylated fatty acids as inhibitors for the corrosion of zinc in acid media. *Mats. Chem. & Phys.* **2005**, *89*(2-3), 183-191. DOI: http://dx.doi.org/10.1016/j.matchemphys.2003.09.055.
26. Pascale, B.; David, J. W.; Donald, A. P.; Michael, L. M. Effect of amines on the surface charge properties of iron oxides. *J. Solution Chem.* **2009**, *38*, 925–945. DOI: http://dx.doi.org/10.1007/s10953-009-9419-y.
27. Noçka, E.; Kaçani, J.; Gaçe, Z. The study of hydrogen permeation in carbon steel and inhibitors impact. *Scientific University of Rousse*. **2008**, *47*(8), 43-48.
28. James, O.O.; Ajanaku, K.O.; Ogunniran, K.O.; Ajani, O.O.; Siyanbola, T.O.; John, M.O. Adsorption behaviour of pyrazolo [3, 4-b] pyridine on corrosion of stainless steel in hcl solutions. *Trends in Applied Sci. Research*, **2011**, *6*(8), 910-917. DOI: http://dx.doi.org/10.3923/tasr.2011.910.917.
29. Felicia, R.S.; Santhanalakshmi, S.; Wilson, S.J.; John, A.A.; Susai, R. Synergistic effect of succinic acid and Zn^{2+} in controlling corrosion of carbon steel. *Bulletin of Elect*. **2004**, *20*(12), 561-565.

30. Obot, I.B.; Obi-Egbedi, N.O. Adsorption properties and inhibition of mild steel corrosion in sulphuric acid solution by ketoconazole: experimental and theoretical investigation. *Corros. Sci.* **2010**, *52*(1), 198–204. DOI: http://dx.doi.org/10.1016/j.corsci.2009.09.002.
31. Abdel-Rehim, S.S.; Khaled, K.F.; Abd-Elshafi, N.S. Electrochemical frequency modulation as a new technique for monitoring corrosion inhibition of iron in acid media by new thiourea derivative. *Electrochim. Acta*. **2006**, *52*(16), 3269-3277. DOI: http://dx.doi.org/10.1016/j.electacta.2005.09.018.
32. Hosseini, M.; Mertens, S.F.L.; Arshadi, M.R. Synergism and antagonism in mild steel corrosion inhibition by sodium dodecylbenzenesulphonate and hexamethylenetetramine. *Corros. Sci.* **2003**, *45*(7), 1473-1489. DOI: http://dx.doi.org/10.1016/S0010-938X(02)00246-9.
33. Villamil, R.F.V.; Corio, P.; Rubim, J.C.; Agostinho, S.M.I. Effect of sodium dodecylsulfate on copper corrosion in sulfuric acid media in the absence and presence of benzotriazole. *J. Electronalytical Chem.* **1999**, *472*(2), 112-119. DOI: http://dx.doi.org/10.1016/S0022-0728(99)00267-3.
34. Abiola, O.K. Adsorption of 3-(4-amino-2-methyl-5-pyrimidyl methyl)-4-methyl thiazolium chloride on mild steel. *Corros. Sci.* **2006**, *48*(10), 3078-3090. DOI: http://dx.doi.org/10.1016/j.corsci.2005.12.001.
35. Bockris, J. O. M. Modern Electrochemistry. London: Macdonald Ltd, 1970; p. 772
36. Damaskin, B.B.; Frumkin, A.N. Adsorption of molecules on electrodes. Wiley-Interscience: London, 1971; p.36
37. Susuki, M. Adsorption Engineering. Elsevier: Amsterdam 1990; p. 52.
38. Li, X.H.; Deng, S.D.; Fu, H.; Mu, G.N. Inhibition by tween-85 of the corrosion of cold rolled steel in 1.0 M hydrochloric acid solution. *J. App. Elect.* **2009**, *39*, 1125-1135. DOI: http://dx.doi.org/10.1007/s10800-008-9770-5.
39. Lowmunkhong, P.; Ungthararak, D.; Sutthivaiyakit, P. Tryptamine as a corrosion inhibitor of mild steel in hydrochloric acid solution. *Corros. Sci.* **2010**, *52*(1), 30-36. DOI: http://dx.doi.org/10.1016/j.corsci.2009.08.039.
40. Susai, R.S.; Mary, R.; Noreen, A.; Ramaraj, R. Synergistic corrosion inhibition by the sodium dodecylsulphate–Zn^{2+} system. *Corros. Sci.* **2002**, *44*(10), 2243-2252. DOI: http://dx.doi.org/10.1016/S0010-938X(02)00052-5.
41. Sahin, M.; Bilgiç, S.; Yılmaz, H. The inhibition effects of some cyclic nitrogen compounds on the corrosion of the steel in NaCl mediums. *App. Surf. Sci*. **2002**, *195*(104), 1-7. DOI: http://dx.doi.org/10.1016/S0169-4332(01)00783-8.
42. Rocca, E.; Rapin, C.; Mirambet, F. Inhibition treatment of the corrosion of lead artefacts in atmospheric conditions and by acetic acid vapour: use of sodium decanoate. *Corros. Sci.* **2004**, *46*(3), 653-665. DOI: http://dx.doi.org/10.1016/S0010-938X(03)00175-6.
43. Tebbji, K.; Oudda, H.; Hammouti, B.; Benkaddour, M.; El Kodadi, M.; Ramdani, A. Inhibition effect of two organic compounds pyridine–pyrazole type in acidic corrosion of steel. *Colloids and Surfs. A: Physicochem. Eng. Asps.* **2005**, *259*, 143-149. DOI: http://dx.doi.org/10.1016/j.colsurfa.2005.02.030.
44. Bockris, J.O.; Swinkels, D.A.J. The relative electrocatalytic activity of noble metals in the oxidation of ethylene. *J. Elect. Soc.* **1964**, *111*(6), 728-736. DOI: http://dx.doi.org/10.1149/1.2426221.
45. Benali, O.; Benmehdi, H.; Hasnaoui, O.; Selles, C.; Salghi, R. Green corrosion inhibitor: inhibitive action of tannin extract of Chamaerops humilis plant for the corrosion of mild steel in 0.5M H_2SO_4. *J. Mats. & Environ. Sci.* **2013**, *4*(1), 127–138.

Article citation:
Loto, R. Corrosion inhibition studies of the combined admixture of 1,3-diphenyl-2-thiourea and 4-hydroxy-3-methoxybenzaldehyde on mild steel in dilute acid media. *Rev. Colomb. Quim.* **2017**, *46* (1), 20-32. DOI: http://dx.doi.org/10.15446/rev.colomb.quim.v1n1.59578.